Big Data
Volume 00, Number 00, 2021

DOI: 10.1089/big.2020.0350

# Evaluating the Impact of Summer Drought on Vegetation Growth Using Space-Based Solar-Induced Chlorophyll Fluorescence Across Extensive Spatial Measures

Sanjeevi Pandiyan,[1] Govindjee Govindjee,[2] S. Meenatchi,[3] S. Prasanna,[3] G. Gunasekaran,[3] and Ya Guo[1,4,*]

**Abstract**

Drought is the primary and dominant natural cause of stress on vegetation, and thus, it needs our full attention. Current understanding of drought across extensive spatial measures, around the world, is considerably limited. As case studies to evaluate the feasibility of utilizing space-based solar-induced chlorophyll fluorescence (SIF) across extensive spatial measures, here, we have used data from 2007 to 2017 in Heilongjiang and Jiangsu provinces of China. The onset of the 2015 drought was accompanied by a substantial response of SIF from vegetation in both the provinces; these data were associated with changes in soil moisture, standardized precipitation evapotranspiration index, and emissivity. Our findings suggest that SIF can effectively provide the spatial and temporal progress of drought, as inferred through substantial associations with SIF normalized by absorbed photosynthetically active radiation (related to $\Phi_F$) and by photosynthetically active radiation ($\mathbf{SIF_{PAR}}$). For the depiction of onset to drought, SIF, $\Phi_F$, and $\mathbf{SIF_{PAR}}$ provide a significant association and a quicker response than the leaf area index and the normalized difference vegetation index. Furthermore, we found that the correlation between gross primary productivity and SIF is highly substantial in both Heilongjiang ($R^2 = 0.85$, $p < 0.001$) and Jiangsu ($R^2 = 0.75$, $p < 0.001$) during the drought period. Our results indicate that continuing evaluation from space-based SIF can indeed provide an understanding of the seasonal differences in vegetation for evaluating the impact of drought across extensive spatial measures.

**Keywords:** solar-induced chlorophyll fluorescence; gross primary production; leaf area index; normalized difference vegetation index; drought; vegetation



## Introduction

Drought (water deficit) is a dominant natural stress on vegetation activity and thus requires our attention;[1,2] also see Pareek et al.[3] Extreme drought can substantially affect water storage, farming cultivation, ecological land systems, and later cause harmful effects on the evolution of economy and civilization.[4] Specifically, when there is global warming and an expanding demand for water through human activities, drought becomes a serious problem.[5] Conceptually, efficient drought tracking across extensive spatial measures is necessary to solve the problems caused by drought.

Drought is associated with either below-average rainfall or above-average air warming, which remains constant for weeks, years, or even several decades; this has significant consequences for vegetation growth. The prevalence and time span of drought have been increasing over time due to climate change.[6–8] Several drought periods are known to have existed within various regions throughout the world, in particular, in north China from 2013 to 2014,[9] in Europe during 2018,[10] in North America from 2011 to 2012,[11] and in temperate areas in Southeast Asia and the Amazon from 2015 to 2016.[12,13]

[1]*Key Laboratory of Advanced Process Control for Light Industry, Ministry of Education, Jiangnan University, Wuxi, China.*
[2]*Department of Plant Biology, Department of Biochemistry, and Center of Biophysics & Quantitative Biology, University of Illinois at Urbana-Champaign, Urbana, Illinois, USA.*
[3]*School of Information Technology and Engineering, Vellore Institute of Technology, Vellore, India.*
[4]*Department of Bioengineering, University of Missouri, Columbia, Missouri, USA.*

*Address correspondence to: *Ya Guo, Department of Bioengineering, University of Missouri, Columbia, MO 65211, USA,* E-mail: guoy@jiangnan.edu.cn; guoy@missouri.edu

The occurrence of intense drought has increased substantially throughout previous decades and had a significant effect on the ecological systems, for example, in southern China.[14,15] The major drought after the fall of 2018 resulted in a financial loss of more than 8 billion US dollars in southwestern China.[16] Furthermore, the 2017 drought in Italy caused increased air warming compared with the long-term mean, breaking all previous records.[17]

Vegetation attributes, obtained through various remote sensing approaches, have been measured to explore the effects of drought on vegetation. Vegetation indices (VIs), such as leaf area index (LAI), and normalized difference vegetation index (NDVI) obtained from the Moderate Resolution Imaging Spectroradiometer (MODIS)[18] have been used to measure the greenness of crops. Below-normal crop greenness was observed during the 2000–2016 drought period, as measured through NDVI,[19] although there has been a difference of opinion on the crop greenness abnormalities during the 2016 drought period.[20] Analysis of these sensor perceptions is problematic as they are severely induced through sun-sensor geometric variations and atmospheric impacts.[21–23]

The NDVI employs visible and near-infrared reflections on two edges, referred to as red edges; furthermore, they are responsive to the measure of the so-called green bioenergy over a space-based pixel.[24] These indicators and their related attributes have been extensively employed to explore physiological changes in vegetation.[25–27]

Space-based assessment of solar-induced chlorophyll fluorescence (SIF) has been available for several years for tracking vegetation worldwide.[28–32] SIF is currently being obtained through various space-based devices, such as Global Ozone Monitoring Instrument-2 (GOME-2),[33] Greenhouse gases Observing SATellite,[34,35] and the Orbiting Carbon Observatory-2 (OCO-2).[36] These devices have their foundation in several ground-based and satellite analyzing systems.[37,38]

SIF measurement is based on the fact that a small amount of absorbed energy is released as fluorescence; this fluorescence has two emission peaks at about 685 and 740 nm,[24] recognized as the red and far-red emission bands. For background on all aspects of chlorophyll fluorescence, see chapters in Papageorgiou and Govindjee[39] and Govindjee et al.[40]

In any environment, a significant portion of the absorbed photosynthetically active radiation (APAR) is used by the photochemical pathway leading to photosynthesis; the actual values depend on various conditions, including temperature. SIF measurements are sensitive to the fraction of APAR (fPAR). SIF captures photosynthesis changes caused by drought; furthermore, published data show that SIF was more sensitive to plant physiological variations.[41,42] The space-based SIF information is highly useful in assessing photosynthesis on local as well as on a worldwide scale.[43] SIF has been utilized for agriculture fidelity over different crop canopies to observe changes in photosynthesis-related process throughout the day.[44]

Furthermore, space-based NDVI can be employed to analyze the association among gross primary productivity (GPP) for exploring the consistency of vegetation.[45,46] Gonsamo et al.[47] compared space-based NDVI information over tower-estimated $CO_2$ flux details with FLUXNET. Few years later, Jeong et al.[48] found that the NDVI-derived drought period was longer in duration than flux metrics, indicating an inconsistency in seasonal pattern among vegetation functionality. This inconsistency may be the result of variations in the measurements among space-based and tower metrics[49]; thus, alternative ways and means are essential to solve these concerns.

Typically, almost 1% of the solar energy acquired through vegetation is retransmitted through chlorophyll as fluorescence (see chapters in Papageorgiou and Govindjee[39] and Govindjee et al.[40]). Phenology-based studies on leaf canopies show a clear association between SIF and photosynthesis.[50,51] Both SIF and GPP are associated with the light absorption process of photosynthesis,[52] and space-based SIF is considered to be the direct reflection of photosynthetic action. Consequently, we must attempt to associate information from space-based SIF data with GPP for validating the seasonal changes in vegetation at the study areas.

The rate of losses in vegetation productivity by drought has been increasing during the past 30 years; furthermore, more than 30 drought cases have been observed once every 2 years during the past 60 years in Heilongjiang province of China.[53] Concurrently, drought rates also showed a rising trend throughout this province. Similarly, there are records of drought events in 13 areas in Jiangsu province of China. It is important to note that, in this province, the water deficit has been above 60%.[54] During June 2011, the affected regions of crops were 401 thousand hectares in Jiangsu, and the direct economic loss was of 1.35 billion Yuan (www.stats.gov.cn).

Furthermore, increases in the frequency and intensity of drought in Heilongjiang and Jiangsu might damage vegetation yield and thus the entire agricultural sector. The spatial and temporal attributes of the agricultural drought hazard in both the provinces were assessed. In our study, we have detected drought conditions over both the provinces during the summer months for 11 years from 2007 to 2017 through measurements of soil moisture (SM), standardized precipitation evapotranspiration index (SPEI), and emissivity (which provides information on the atmospheric column water vapor and lower boundary air surface temperature).

In addition, we have analyzed the impact of drought on vegetation growth through LAI, SIF, SIF normalized by APAR ($\Phi_F$), SIF normalized by PAR ($SIF_{PAR}$), and NDVI. The associations among SIF and SM, SPEI, and emissivity can advance the insight of drought over Heilongjiang and Jiangsu. The goal of our current study was to: (1) investigate the spatiotemporal evolution of the drought event across extensive spatial measures; (2) evaluate the relationship and responses of SIF and traditional VIs to drought in both the provinces; and (3) explore the interannual changes of LAI, SIF, $\Phi_F$, $SIF_{PAR}$, and NDVI for the summer period in both provinces.

## Data and Methods

### Study area

Heilongjiang province is located between 121°130′–135°05′E in longitude and 43°22′–53°24′N in latitude (Fig. 1a). This northern province of China has an area of 454,000 $km^2$ and a population of more than 38.17 million people. The yearly temperature in Heilongjiang has been between −4 and 4°C, and the annual precipitation has averaged over 500–600 mm. In this province, the mountainous regions account for 59% of the land. Referred to as the "Great northern granary," Heilongjiang province produced more than 43.5 million tons of grain in 2009 from 2.85 million ha of agricultural land. The entire province is situated in the mid-temperate climate zone and is prone to drought.

Jiangsu province is located in the eastern part of China within the longitudes 116°18′–121°57′ E and the latitudes 30°45′–35°20′ N covering an area of

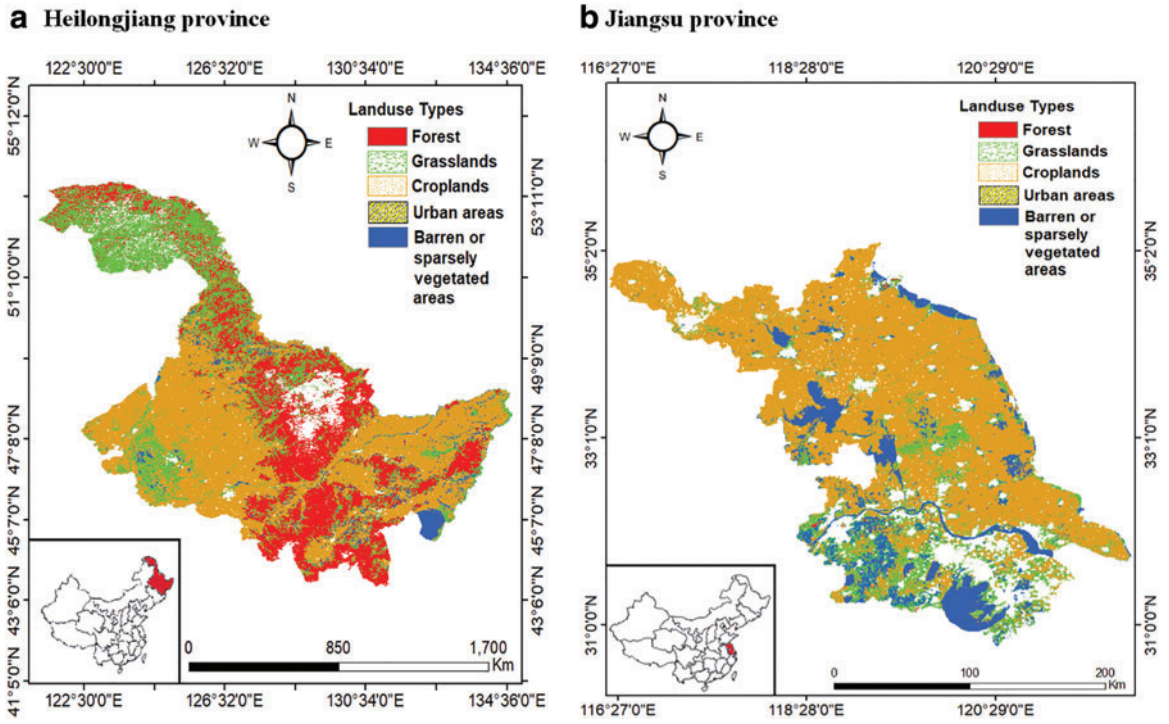


**FIG. 1.** Distribution of dominant vegetation types in Heilongjiang province **(a)** and Jiangsu province **(b)** based on MODIS vegetation product data. MODIS, Moderate Resolution Imaging Spectroradiometer. Color images are available online.

around 100,000 km$^2$ (Fig. 1b). Water bodies, grasslands and hills, and mountains, respectively, make up 16.8%, 68.0%, and 14.3% of the entire territorial province. The typical yearly precipitation ranges between 550 and 1450 mm, which is highest in the summers. Its population of 78.5 million inhabitants makes Jiangsu province the most densely populated territory in China (www.stats.gov.cn). The most severe drought recorded in the past 50 years was in 2011.[55] This damaging effect led to an increased interest in the tracking and evaluation of the ecosystem resulting from drought activity.

## Data

**Moisture calculation in soil and SPEI.** To assess the impact of distinct drought events on vegetation development in Heilongjiang and Jiangsu, SM at 0.25° soil information ESA CCI SM v04.4 (https://www.esa-soilmoisture-cci.org) was used in our study. To detect the effects of drought patterns on vegetation development, SM resources were assessed during 2007–2017. SM data indicate precipitation irregularities, and we used them to represent the spatial anomalies of drought in both Heilongjiang and Jiangsu provinces.

Vicente-Serrano et al.[56] had already considered SPEI for comparing evapotranspiration variables with temperature. SPEI has numerous advantages in drought detection, and thus, it was used in our present study. The monthly SPEI information was acquired at a spatial resolution of $1° \times 1°$ by using an SPEI global drought monitor (http://spei.csic.es). To fit and equalize the spatial resolution of additional information, all the data were incorporated into the latitudinal dimension of $0.5° \times 0.5°$. Furthermore, SPEI was used in Heilongjiang and Jiangsu provinces for assessing the past scarcity of water and severity and their associations to the drought.

**Data products of MODIS.** We utilized MODIS data products, which included emissivity, GPP, fPAR, surface reflectance, LAI, and NDVI (https://lpdaac.usgs.gov). The MOD17A2H (V6) GPP, an 8-day composite of scales through a 500-meter (m) pixel size, was used to explore the water cycle processes of the vegetation. Furthermore, the MOD21A2 (V6) of MODIS, an 8-day composite data set, was used to acquire emissivity from the MODIS thermal infrared bands through the optimal water vapor scaling atmospheric correction pattern. Reflectance-grounded vegetation directories, including LAI and NDVI, were employed to assess the response of drought during vegetation growth. The MCD15A2H (V6) of MODIS, Level 4 of the composite data set, was used to derive LAI. The 500-meter pixel size LAI data set was utilized to acquire the one-sided green leaf area per unit ground area in broadleaf canopies during the period from 2007 through 2017. The NDVI-MODIS product was used from MOD13A3 (V6) to understand the drought-related vegetation growth conditions.

**GOME-2 solar-induced chlorophyll fluorescence.** In this study, we have utilized information (Level 3, V28) (https://avdc.gsfc.nasa.gov), provided through the GOME-2. MetOp-A/B was associated through GOME-2 programs that have an equator passage spell at 09:30 a.m. In the spectral range of 600–800 nm, GOME-2 provided radiance of about 740 nm and was used for SIF through the principal component analysis method, as performed by Joiner et al.[57] and Frankenberg and Berry[58] More than 50% was lost when going through a cloud segment, as shown by Köhler et al.[59] SIF responses were combined with data from monthly resources at $0.5° \times 0.5°$ and a minimum of five SIF retrievals in 30 days were obtained. Here, we investigated this robust association between SIF and VIs through the vegetation composition. We characterize this as shown below[60]:

$$\mathrm{SIF} = \mathrm{PAR} * \mathrm{fPAR} * \Phi_F * \Omega_C, \tag{1}$$

$$\Phi_F = \frac{\mathrm{SIF}}{\Omega_C * \mathrm{APAR}} = \frac{\mathrm{SIF}_{\mathrm{PAR}}}{\mathrm{fPAR}}, \tag{2}$$

$$\mathrm{SIF}_{\mathrm{PAR}} = \frac{\mathrm{SIF}}{\Omega_C * \mathrm{PAR}}, \tag{3}$$

where $\mathrm{SIF}_{\mathrm{PAR}}$ is SIF regulated through photosynthetically active radiation, and PAR is the occurrence flux of APAR and remains a segment for fPAR, which was obtained by the data products of MODIS (MOD15 A2), $\Omega_C$ is an escape eventuality binding the discharge of fluorescence from the top of the canopy to the emission of fluorescence at the level of the chloroplast membranes[24]; $\Phi_F$ is the yield of fluorescence in the wavelength band of the measures and signifies the efficiencies for chlorophyll fluorescence emission, respectively.

## Results

### Interannual anomalies in SM, SPEI, and emissivity

We initially considered the interannual anomalies of the SM, SPEI, and emissivity within Heilongjiang and Jiangsu provinces for the summer periods during 2007–2017, as shown in Figure 2. In both Heilongjiang and Jiangsu, SM, SPEI, and emissivity indicate significant interannual dissimilarities. In June, for all the years (2007–2017) examined, SM remained higher than the mean in Heilongjiang than in Jiangsu. In comparison to SM and emissivity, negative SPEI anomalies were noted in 2007, 2008, 2010, and 2013 for Heilongjiang province, and in 2010, 2012, 2013, 2014, 2015, and 2017 for Jiangsu province. In July 2011, the mean values of SPEI and emissivity remained lower in Heilongjiang than in Jiangsu. All these three (SM, SPEI, and emissivity) parameters show a drought-associated reduction in 2015 compared with those during 2007–2017 in both the provinces during the vegetation growth. Consequently, we focused on the drought case in the summer 2015 for further analysis.

### Spatial distributions of SM, SPEI, and emissivity during 2015 drought in Heilongjiang

The monthly spatial allocation of the SM, SPEI, and emissivity in Heilongjiang was acquired, in 2015, from June to August (Fig. 3). Generally, the spatial allocation of the SM fluctuated with increases and decreases in the monthly SPEI. SM in the northern region of Heilongjiang province, during the month of June, had severely decreased since there was no precipitation for 2 months before it. This change is indicated much more clearly in SM mapping during July and August, as the measures change from $-0.05$ to 0.02 $m^3m^{-3}$, showing that a significant drought had occurred in June. Data on the mean assesses of surface SM of Heilongjiang showed a gradual incline indicating drought during June.

The response of the SPEI transit over the zero-scale range reflected a dry-wet state during August in Heilongjiang. Additionally, the occurrence of the drought was higher in the central regions of the province during July. The spatial SPEI increased slightly in June but declined in July. The observed emissivity during the summer drought decreased as the time scale increased. The frequency of emissivity in June and August was within 15%–25%, and the frequency in July in the eastern part of Heilongjiang was less compared with that in the northern region of this province.

### Spatial distributions of SM, SPEI, and emissivity during 2015 drought in Jiangsu

The spatial distributions of the SM, SPEI, and emissivity in Jiangsu, acquired from June to August 2015, are shown in

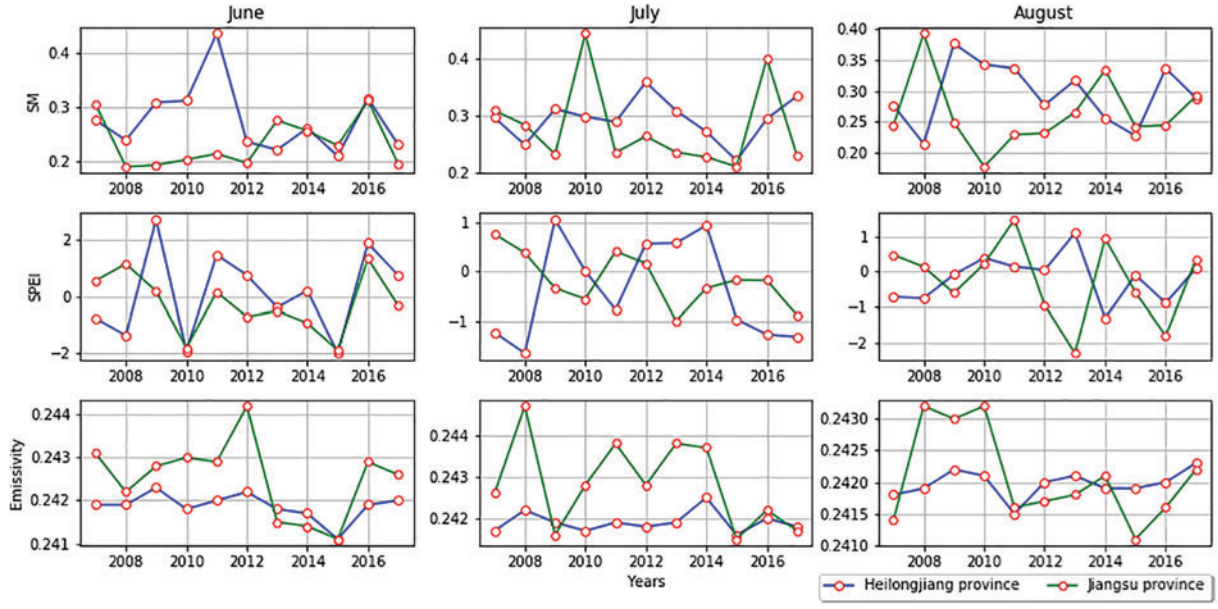


**FIG. 2.** Interannual changes of SM, SPEI, and emissivity for the summer (June–August) periods during 2007–2017 in Heilongjiang and Jiangsu. SM, soil moisture; SPEI, standardized precipitation evapotranspiration index. Color images are available online.

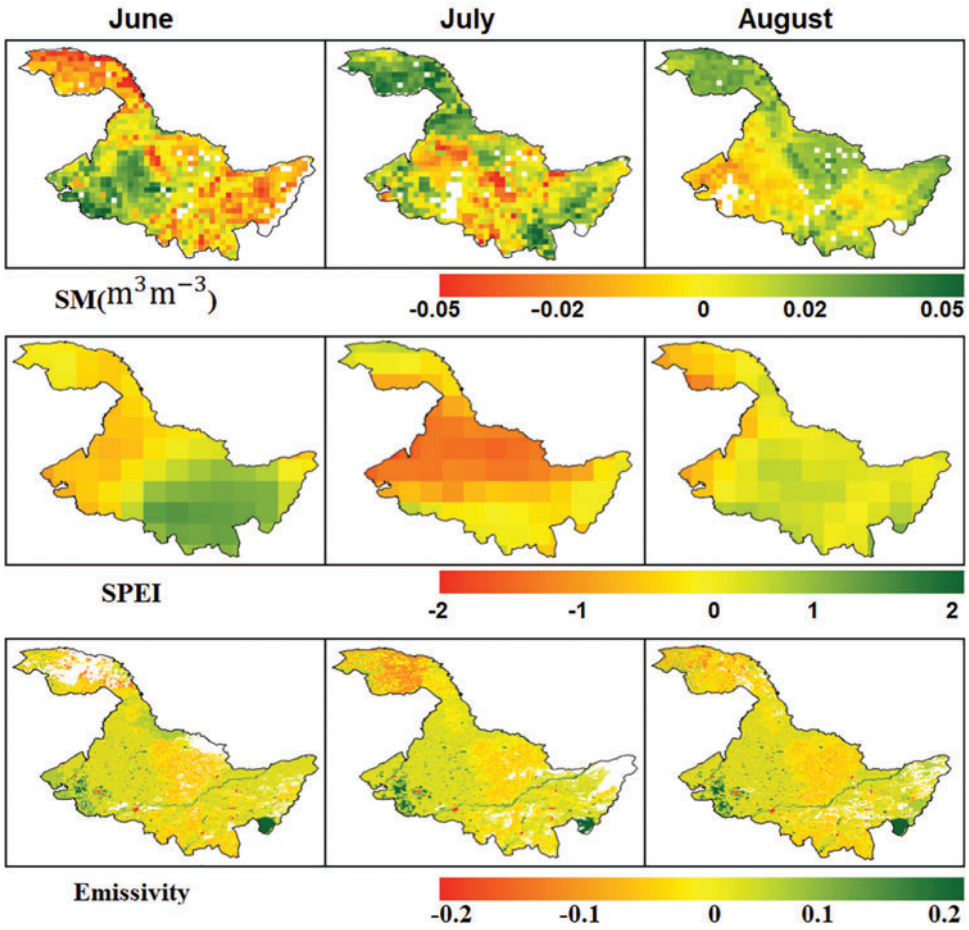


**FIG. 3.** The spatial distribution of the anomalies in SM, SPEI, and emissivity in Heilongjiang during the 2015 summer (June–August) period. Color images are available online.

Figure 4. The SM anomaly indicates less variation with less amplitude in the summer months, where the average SM anomaly was 0.02 $m^3m^{-3}$. The SM measures in August show much more negative anomaly than in June and July. Generally, the northwest area of Jiangsu is moderately dry compared with the central and eastern parts, which reflects the precipitation gradient across Jiangsu province.

The majority of the province during June showed low SPEI (e.g., between −1 and 1 [80%] in the north and northwest areas of Jiangsu). For the central regions of the province and some regions in the south, SPEI ranged between 1 and 2 during July. There were some regions with SPEI exceeding 1 throughout August, compared with that in June. Especially, emissivity data for July showed negative anomalies when adequate solar radiation was present, and SM changed indicating significant stress in vegetation growth. In August, there was a lower correlation than in June, which further indicates that a summer drought had occurred in Jiangsu province.

### Interannual anomalies in LAI, SIF, $\Phi_F$, $SIF_{PAR}$, and NDVI

The interannual anomalies of LAI, SIF, $\Phi_F$, $SIF_{PAR}$, and NDVI over the drought periods during June–August from 2007 to 2017 were analyzed (Fig. 5). In both the provinces, studied here, the space-based perceptions of LAI are lower compared with the multi-annual average in June 2008, when the SM, SPEI, and emissivity changed due to precipitation scarcity. In June, the measures of LAI in Heilongjiang were nearly equal to the multi-annual average, and the measures of NDVI were significantly higher than multi-annual average.

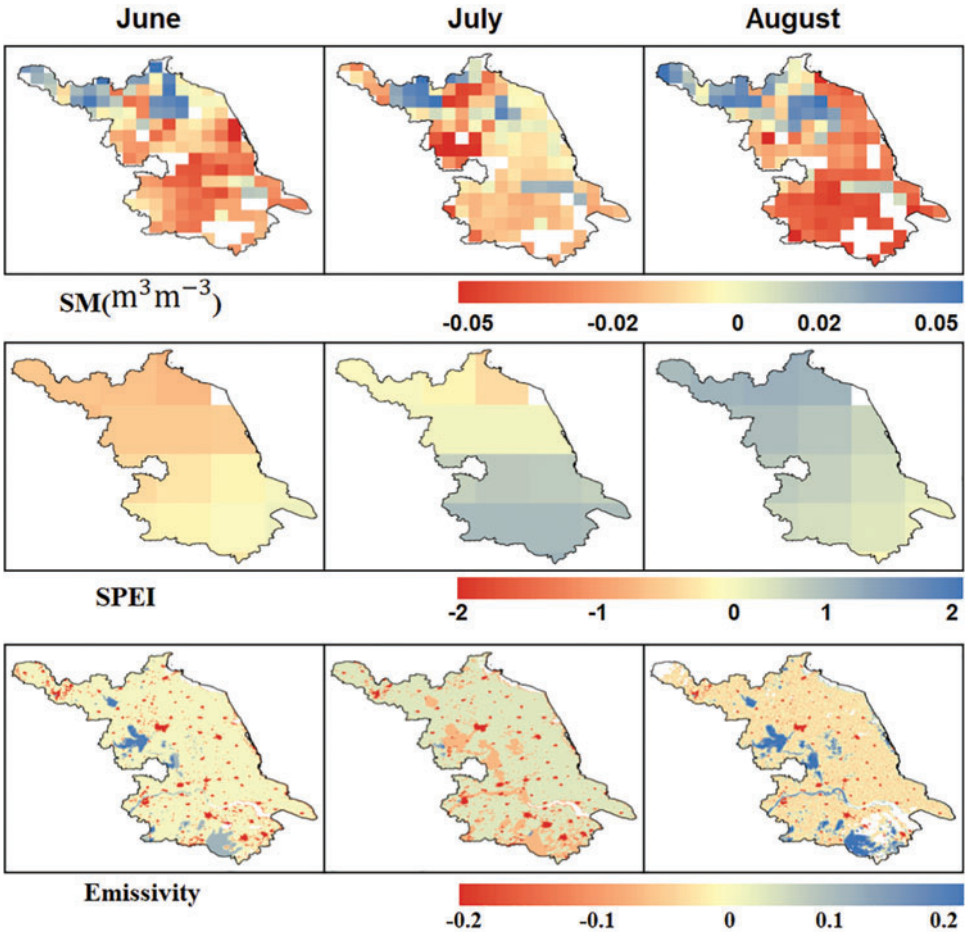


**FIG. 4.** The spatial distribution of the anomalies of SM, SPEI, and emissivity in Jiangsu during the 2015 summer (June–August) period. Color images are available online.

While drought expanded through the province, LAI and NDVI showed a moderately poor response to drought in July. However, SIF, $\Phi_F$, and $SIF_{PAR}$ indicated significantly higher sensitivity and much more constant reduction in response to drought than LAI and NDVI. Similarly, measures of SIF, $\Phi_F$, and $SIF_{PAR}$ in Jiangsu province showed a substantial reduction in July and August compared with the multi-annual average, showing that there was a consistent response of vegetation to drought. Overall, the study of both provinces shows that SIF, $\Phi_F$, and $SIF_{PAR}$ indeed reflect drought dynamics and are much more sensitive to severe drought environments than LAI and NDVI.

### Spatial distributions of LAI, SIF, $\Phi_F$, $SIF_{PAR}$, and NDVI during 2015 drought in Heilongjiang

The spatial distribution of LAI, SIF, $\Phi_F$, $SIF_{PAR}$, and NDVI during 2015 was investigated to study the vegetation responses to drought in Heilongjiang (Fig. 6). Over the severe drought event, SIF, $\Phi_F$, and $SIF_{PAR}$ show a sudden reduction in June, and the LAI and NDVI outset in June and increased in July and August indicating a delayed response to drought.

The major part of the province shows positive anomalies of LAI and NDVI in June at the onset of the drought. However, 60%–70% of this province had positive SIF, $\Phi_F$, and $SIF_{PAR}$ anomalies. While drought increased in Heilongjiang, more than 35% of the vegetation in the province reflected mild losses of $SIF_{PAR}$ in July, and more than 20% of the vegetation suffered severe losses. Furthermore, the proportion of mild and severe $\Phi_F$ loss was 19% and 36%, respectively.

In contrast, only 32% and 9% of the province showed slight and severe LAI loss. The greater part of Heilongjiang experienced drought, as indicated through data

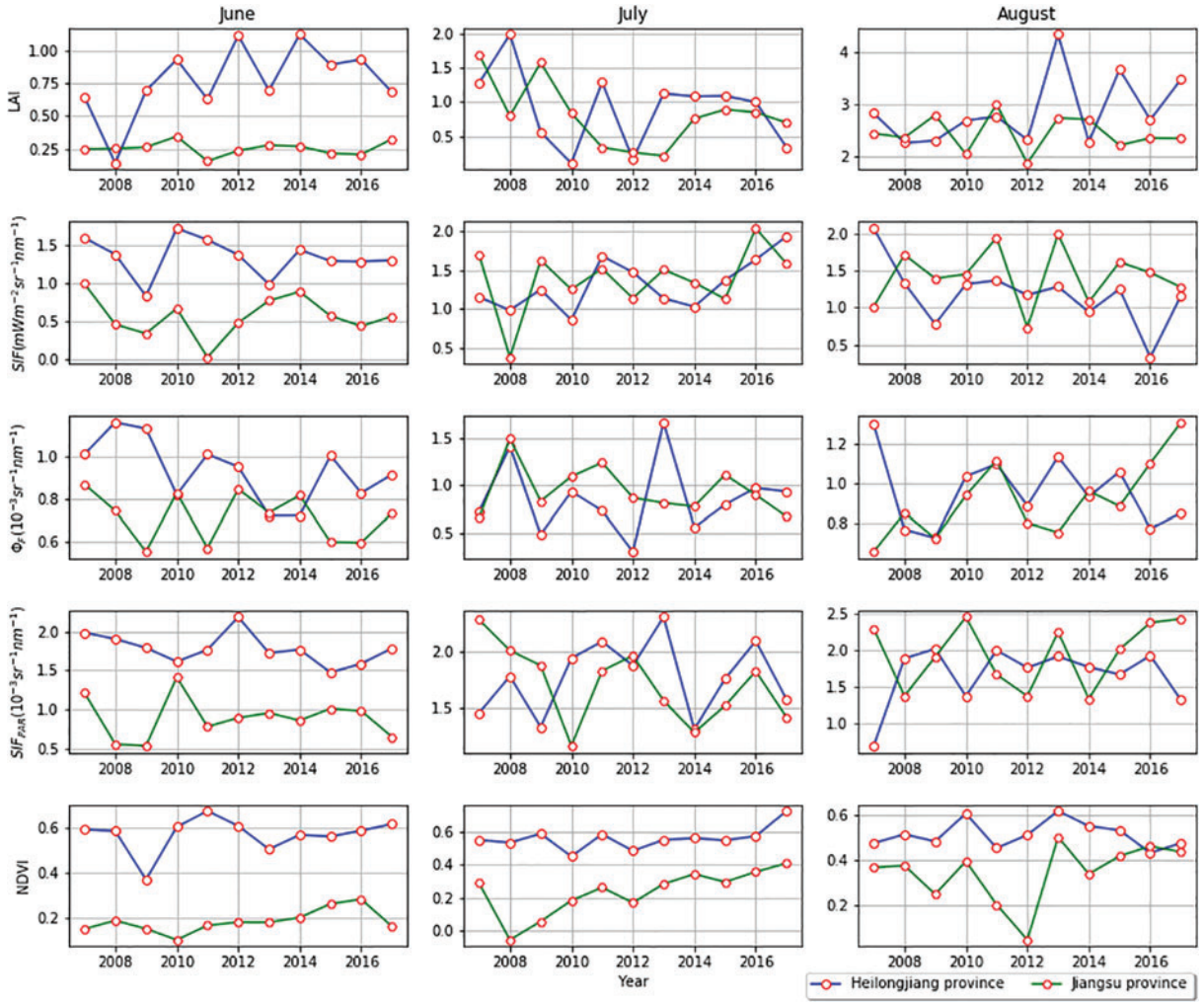


**FIG. 5.** Interannual changes of LAI, SIF, $\Phi_F$, $SIF_{PAR}$, and NDVI for the summer (June–August) period 2007–2017 in Heilongjiang and Jiangsu. APAR, absorbed photosynthetically active radiation; LAI, leaf area index; NDVI, normalized difference vegetation index; PAR = photosynthetically active radiation; SIF, solar-induced chlorophyll fluorescence; $SIF_{PAR}$, SIF normalized by PAR; $\Phi_F$, SIF normalized by APAR. Color images are available online.



on LAI, $\Phi_F$, and $SIF_{PAR}$, in August, while LAI consistently demonstrated fewer anomalies than NDVI. The negative NDVI anomalies manifested largely in the province during July and August. The spatial distributions suggest that SIF, $\Phi_F$, and $SIF_{PAR}$ had larger sensitivity to drought compared with LAI and NDVI.

### Spatial distribution of LAI, SIF, $\Phi_F$, $SIF_{PAR}$, and NDVI during 2015 drought in Jiangsu

The spatial distribution of LAI, SIF, $\Phi_F$, $SIF_{PAR}$, and NDVI during 2015 was investigated to study the vegetation responses to drought in Jiangsu (Fig. 7). SIF, $\Phi_F$, and $SIF_{PAR}$ anomalies were lower in July than in August and also showed lower measures of SM, SPEI, and emissivity (as shown above in Fig. 4), which indicates that vegetation growth can be severely exacerbated through drought in this province.

The mean of $SIF_{PAR}$ during June 2015 is close to the mean of SIF during July 2015, which indicates the precision of drought. Through the advancement of drought, more than 28% of the vegetation in Jiangsu experienced average losses as shown by changes in SIF, $\Phi_F$, and $SIF_{PAR}$. In August 2015, the major part of Jiangsu showed more than 80% negative LAI and

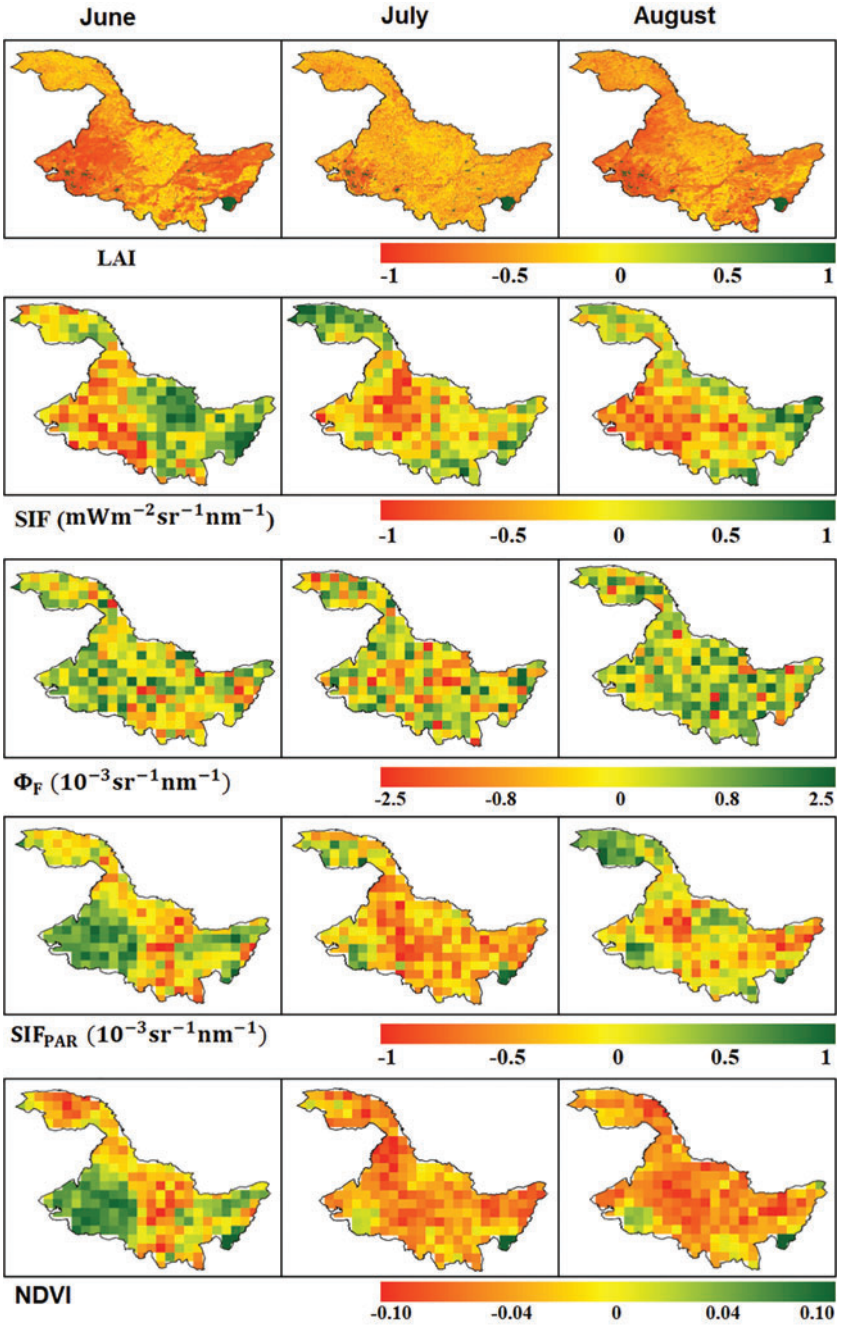


**FIG. 6.** The spatial distribution of the anomalies of LAI, SIF, $\Phi_F$, $SIF_{PAR}$, and NDVI in Heilongjiang province during the 2015 summer (June–August) period. Color images are available online.

NDVI anomalies, and around 45% negative anomalies in SIF, $\Phi_F$, and $SIF_{PAR}$. Moreover, above 18% of the vegetation showed an extreme loss in June.

However, most of Jiangsu province exhibited negative NDVI anomalies in July. As the drought extended, around 75% of Jiangsu province was affected, as identified through changes in SIF, $\Phi_F$, and $SIF_{PAR}$ measures in June and August, although only 30% and 49% of the province had losses in LAI and NDVI. The spatial allocation of LAI and NDVI anomalies

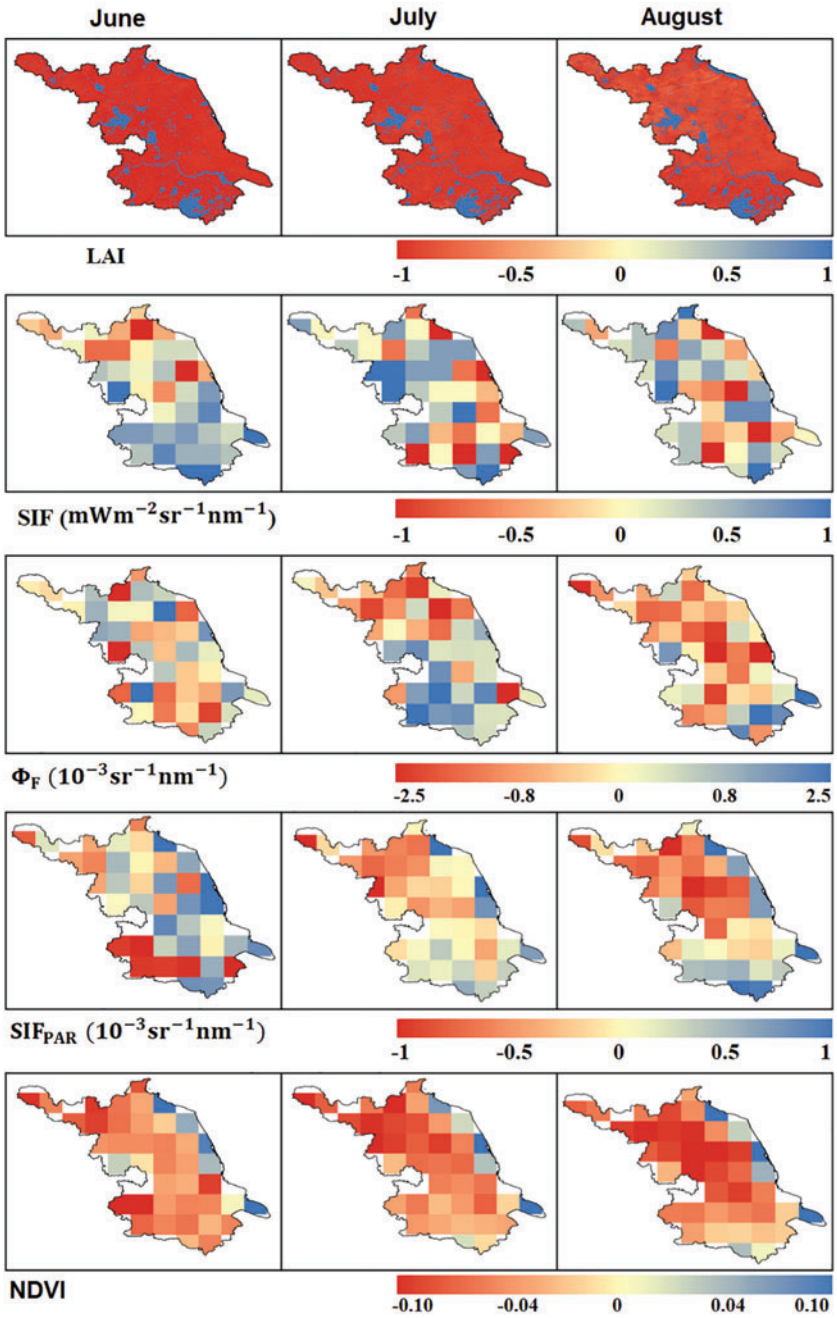


**FIG. 7.** The spatial distribution of the anomalies of LAI, SIF, $\Phi_F$, $SIF_{PAR}$, and NDVI in Jiangsu province during the 2015 summer (June–August) period. Color images are available online.

suggest that the satellite insights of VIs are less sensitive to drought than SIF, $\Phi_F$, and $SIF_{PAR}$. LAI anomalies were negative across the major part of the province and higher in June. However, changes in SIF, $\Phi_F$, and $SIF_{PAR}$ reflect a much more sensible spatial indication of drought than LAI and NDVI.

### Correlation of SM, SPEI, and emissivity with LAI, SIF, $\Phi_F$, $SIF_{PAR}$, and NDVI

Figure 8 shows the correlation of SM, SPEI, and emissivity with LAI, SIF, $\Phi_F$, $SIF_{PAR}$, and NDVI. The impact of drought on SM, SPEI, and emissivity was identical to that on SIF, $\Phi_F$, and $SIF_{PAR}$ during June

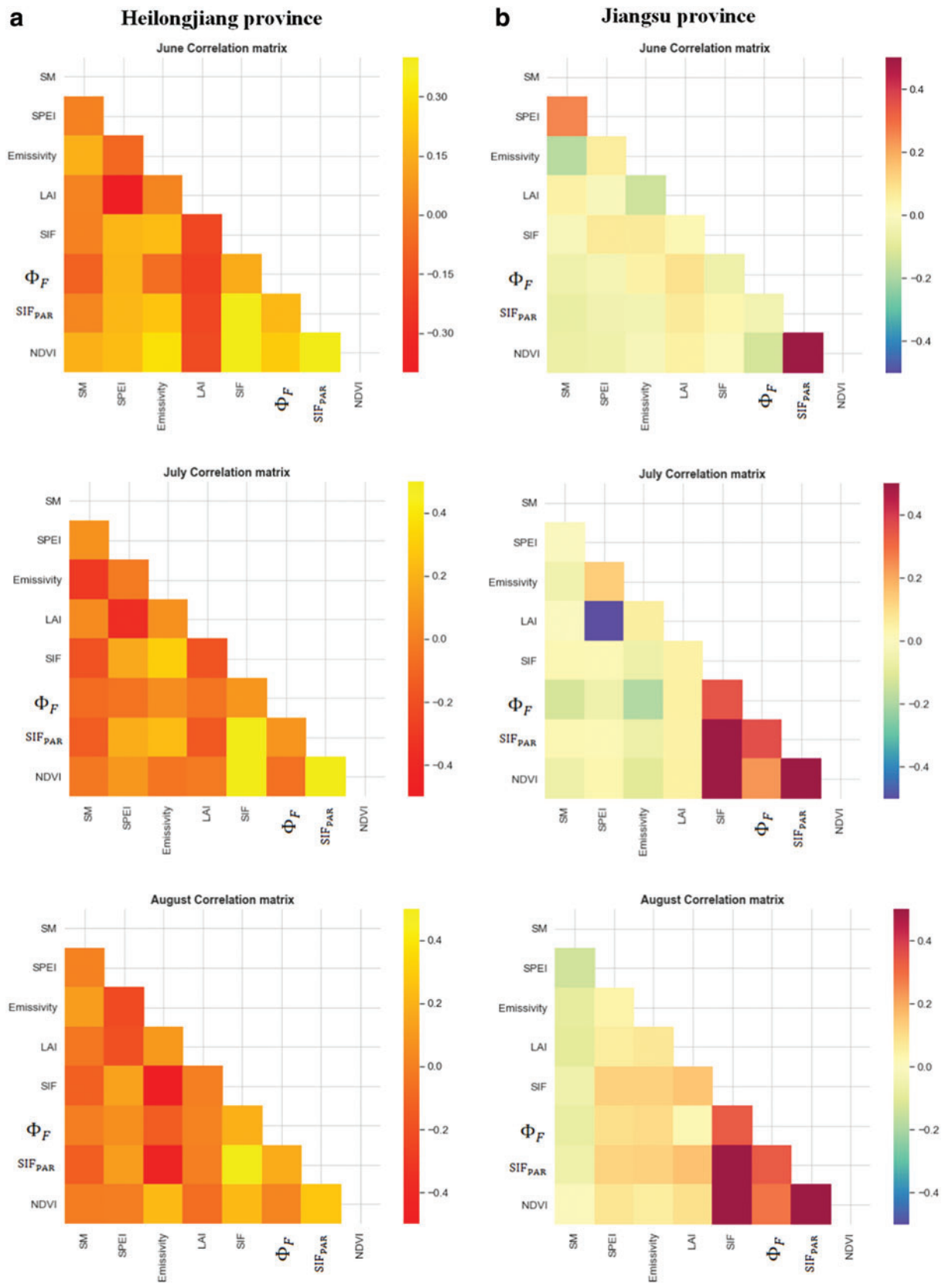


**FIG. 8.** Correlation of SM, SPEI, and emissivity with LAI, SIF, $\Phi_F$, $SIF_{PAR}$, and NDVI in Heilongjiang province **(a)** and Jiangsu province **(b)** during the 2015 summer (June–August) period. Color images are available online.

2015 in both the provinces. In particular, the effects of SPEI on LAI showed a negative correlation during July than during June and August. Direct representations in June 2015 were exploited to evaluate the summer crop output in Heilongjiang, where emissivity and the SIF information can be associated throughout the drought period.

Furthermore, emissivity showed low correlation with LAI during the June–August drought, which was most likely based on the dissimilarity of emissivity with SIF, $\Phi_F$, and $SIF_{PAR}$. SPEI was further covariant and indicated a positive correlation with SIF during June–August in both the provinces studied in this work.

In contrast, SM indicated a lower correlation between LAI and NDVI, which showed that SM was a significant parameter in detecting anomalies in SIF, $\Phi_F$, and $SIF_{PAR}$. During August 2015, the impact of all VIs was insubstantial excluding LAI and NDVI, which, in turn, had indicated a strong correlation with emissivity. SIF, $\Phi_F$, and $SIF_{PAR}$ showed much more substantial correlation with SM and emissivity than LAI and NDVI, emphasizing their significant role in detecting drought. SM, SPEI, and emissivity were substantial in showing the anomalies in SIF, and indeed, NDVI was essential in revealing anomalies in emissivity. SM, SPEI, and emissivity are much more prominent vegetation growth parameters in tracking the anomalies of SIF, $\Phi_F$, and $SIF_{PAR}$ since they showed strong correlations during drought.

### Relationship between SM, SPEI, and emissivity to SIF in the summer months of 2015

Figure 9 shows correlation of SIF with SM, SPEI, and emissivity from data in the summer months of 2015. The observed evaluation indicates that for SM measures lower than 0.2 $m^3m^{-3}$ higher SIF correlations and significant positive slopes are present in both provinces. The correlation between SM and SIF is relatively strong, showing positive slopes by the measures in Heilongjiang ($R^2 = 0.73$, $p < 0.05$) and Jiangsu ($R^2 = 0.75$, $p < 0.05$).

For the SPEI, SIF increased substantially and showed positive correlation in Heilongjiang ($R^2 = 0.81$, $p < 0.05$) and Jiangsu ($R^2 = 0.71$, $p < 0.05$). This information may be (and has been) used through high-intensity farming methods in major parts of both the provinces studied in this article; this is true for substantial cultivation and higher vegetation yield changes, which restore high photosynthetic yield for larger SM.

Moreover, there are clear associations between SIF and emissivity. The positive correlation of SIF for a change in emissivity is greater across the measures in both Heilongjiang ($R^2 = 0.72$, $p < 0.05$) and Jiangsu ($R^2 = 0.77$, $p < 0.05$). The SIF-SPEI correlation has been shown to be significantly stronger compared with the measures of SM and emissivity in Heilongjiang, whereas SIF-emissivity correlation has been shown to be stronger compared with SM and SPEI in Jiangsu, specifically during the drought period (Fig. 9b).

### Relationship between GPP and SIF

Figure 10 shows scatter maps of GPP with SIF during the summer of 2015 in both Heilongjiang and Jiangsu. Significant linear correlations were found between GPP and annual mean SIF in Heilongjiang ($R^2 = 0.85$) and Jiangsu ($R^2 = 0.75$). In 2015, GPP-negative anomalies onset was in June for Heilongjiang, whereas SIF anomalies were significant in July for both the provinces. The SIF-GPP relationship had a relatively stronger correlation in Heilongjiang province compared with Jiangsu province. High GPP values were found in some agricultural regions in the summers. SIF remained clearly associated with GPP, demonstrating that SIF has a high potential in detecting increases in photosynthesis, which is a benefit in assessing vegetation growth during drought across the extensive spatial measure.

## Discussion

An appropriate and precise evaluation of drought stress is needed for tracking threats to terrestrial environment. To advance the level of our understanding regarding measures of drought, the temporal and spatial changes in SIF over the drought periods in Heilongjiang and Jiangsu provinces were evaluated. Our findings show that both LAI and NDVI exhibit a weaker response than SIF, $\Phi_F$, and $SIF_{PAR}$ to the onset of drought (Fig. 5), suggesting that the former two indices are less sensitive to ecological stress, such as drought. Limited research (see e.g., Joiner et al.[57]) has shown that photosynthesis in rainforest parts declines during water stress periods, although crop greenness remains constant. These traditional VIs reflect only potential photosynthesis, but they are not, unfortunately, directly related to the drought analysis approach.

Through correlation analysis, we have found that SIF, $\Phi_F$, and $SIF_{PAR}$ are much more sensitive to severe drought than LAI and NDVI (Fig. 8). This is also the case with the results of Li et al.,[61] who had associated

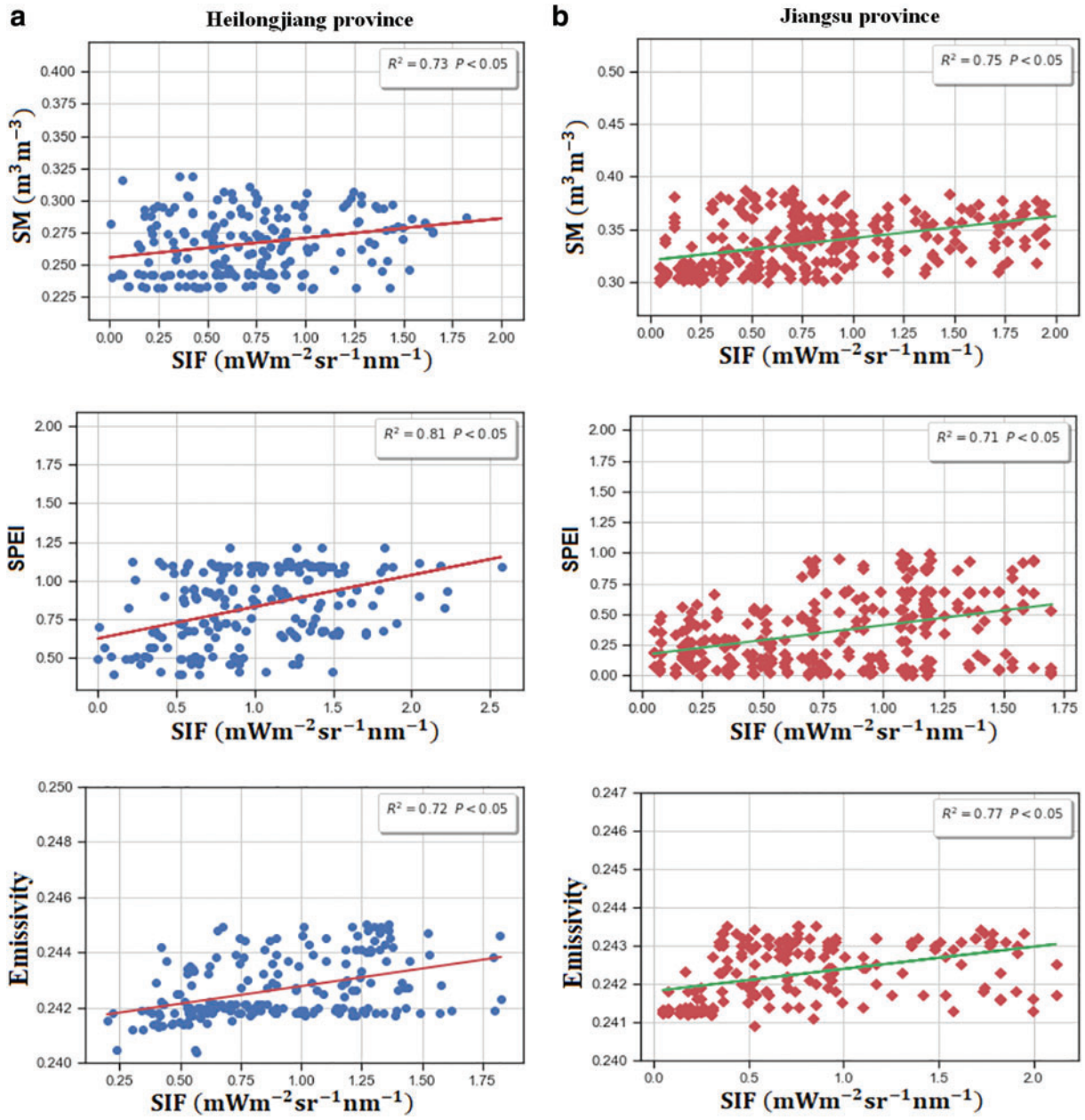


**FIG. 9.** Scatter plots of SM, SPEI, and emissivity to SIF in Heilongjiang **(a)** and Jiangsu **(b)** in the summer months of 2015. Color images are available online.

the effects of drought across the Amazon forest on enhanced vegetation index (EVI) and SIF. Although SIF in the Central Amazon declined much more substantially during moderate dry time spans than during wet time spans, yet EVI indicated only mild changes. Furthermore, we note that the various responses of LAI and NDVI to the progress of drought may be precisely identified through the association of the average measures of SM, SPEI, and emissivity. Thus, further research is needed to exploit all the available parameters.

The analysis of summer drought using SIF across extensive spatial measures during 2007–2017 has provided us key insight and understanding on the relationship of SIF to the evaluation of drought. The findings of our study indicate that SIF response is quicker in providing information on the onset of drought in both

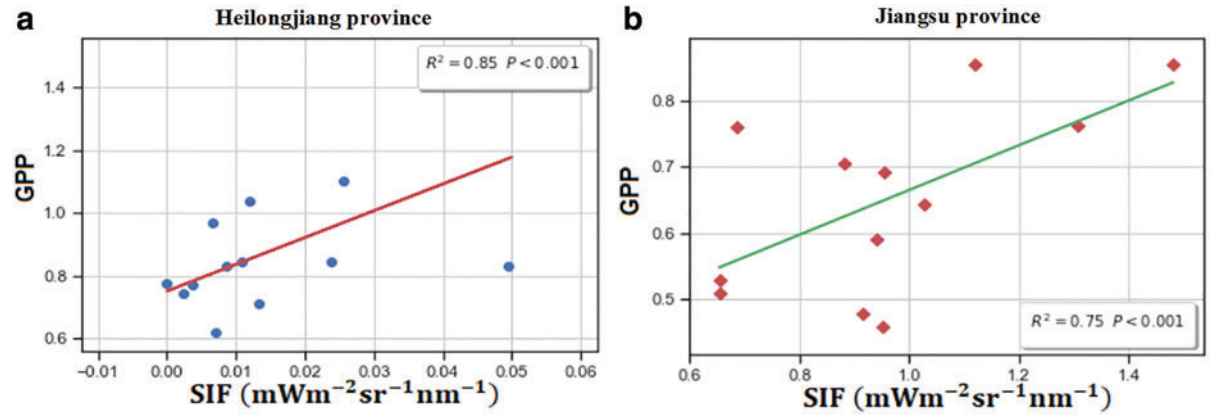


**FIG. 10.** Scatter plots of GPP and SIF in Heilongjiang province **(a)** and in Jiangsu province **(b)** in the summer months of 2015. All relationships are statistically significant ($p < 0.001$). GPP, gross primary productivity. Color images are available online.

Heilongjiang and Jiangsu provinces (Fig. 5). This finding was additionally exploited through the association of SM, SPEI, emissivity with LAI, SIF, $\Phi_F$, $SIF_{PAR}$, and NDVI in both Heilongjiang and Jiangsu (Fig. 9). Specifically, in comparison to NDVI, LAI showed slightly better correlation with SM, SPEI, and emissivity in Jiangsu but slightly weaker correlation in Heilongjiang during June 2015 (Fig. 8).

The variations in the delayed response of LAI and NDVI to SM, SPEI, and emissivity are related to the variations of vegetation demands, such as that of chlorophyll, and its development frequency, and are affected by weather conditions weeks before the measurements. In this context, Yoshida et al.[24] have indicated that SIF and NDVI within mixed forest environments show slight decreases under drought. This signifies that vegetation patterns can also have impact on signals of SIF and NDVI to drought. In conclusion, our study has shown that SIF, $\Phi_F$, and $SIF_{PAR}$ anomalies can be much more effectively used to learn about advancement of drought than traditional VIs.

The scatter plots of GPP and SIF in 2015 are nearly identical (Fig. 10) and show substantial positive correlation in both the provinces examined. This association indicates that GPP is consistent with SIF data in Heilongjiang ($R^2 = 0.85$, $p < 0.001$) and Jiangsu ($R^2 = 0.75$, $p < 0.001$) and is much more precise than in the existing studies from North America.[62] Few regions, specifically in Jiangsu province, compared with Heilongjiang province, had higher SIF measures that were not included in the mapping of GPP. The predominant cause for this poor correlation is that extreme photosynthesis typically occurs within the most appropriate climate state, which may not be reflected in climate data.

Moreover, both provinces studied here have typically sustained regular cloud cover that might have constrained the computation of VIs. However, the SIF data are still noisy, and there are lesser number of measurements in a small number of areas within both the provinces. It is essential that subsequent future research employs SIF and reflectance information at higher spatial and temporal resolution for improved global phenological understanding.

## Conclusions

We have explored the response of SIF over the 2015 drought event in Heilongjiang and Jiangsu provinces of China. For both the provinces, space-based SIF, $\Phi_F$, and $SIF_{PAR}$ had a much higher correlation with drought stress compared with that by LAI and NDVI. Space-based SIF, $\Phi_F$, and $SIF_{PAR}$ show a much more significant response to SM, SPEI, and emissivity than LAI and NDVI during the 2015 drought period. The quick and distinct response of SIF, described in this article, shows high susceptibility to droughts during the vegetation growth period. In this article, we have additionally explored and associated the responses of SM, SPEI, and emissivity to SIF during drought for Heilongjiang and Jiangsu provinces.

We have observed that LAI and NDVI had more distinct delayed responses than SIF, $\Phi_F$, and $SIF_{PAR}$ during the drought period. The spatial, as well as temporal,

paradigms show that the insight obtained from SIF to drought was much more useful compared with that from LAI and NDVI during the 2015 drought event in both the provinces examined in this article. Additionally, we found that SIF anomaly has a much more significant association with the GPP anomaly during the drought period in both Heilongjiang ($R^2 = 0.85$, $p < 0.001$) and Jiangsu ($R^2 = 0.75$, $p < 0.001$) provinces. Thus, SIF offers researchers a powerful tool for precisely tracking the drought across extensive spatial measures.

## Acknowledgment

We are highly thankful to Dr. Nancy Kiang, NASA (National Aeronautics and Space Administration), USA, for reading our article and for her suggestions.

## Author Disclosure Statement

No competing financial interests exist.

## Funding Information

This research was financially supported by the National Natural Science Foundation of China (nos.: 31771680 and 51961125102), the 111 Project (B12018), and Postdoctoral research fund (1255210162190560) from the Jiangnan University.

## References

1. Diaz V, Perez GAC, Van Lanen HAJ, et al. An approach to characterise spatio-temporal drought dynamics. Adv Water Resour. 2020;137:103512.
2. Vicente-Serrano SM, Quiring SM, Peña-Gallardo M, et al. A review of environmental droughts: Increased risk under global warming? Earth-Sci Rev. 2020;201:102953.
3. Pareek A, Sopory SK, Bohnert HJ, et al. Abiotic stress adaptation in plants: Physiological, molecular and genomic foundation. Dordrecht: Springer. 2020. p. 526. ISBN 978-90-481-3111-2; Library of Congress Control Number: 2009941298.
4. Liu L, Yang X, Zhou H, et al. Evaluating the utility of solar-induced chlorophyll fluorescence for drought monitoring by comparison with NDVI derived from wheat canopy. Sci Total Environ. 2018;625:1208–1217.
5. Bai X, Shen W, Wu X, et al. Applicability of long-term satellite-based precipitation products for drought indices considering global warming. J Environ Manage. 2020;255:109846.
6. Nguvava M, Abiodun BJ, Otieno F. Projecting drought characteristics over East African basins at specific global warming levels. Atmos Res. 2019; 228:41–54.
7. Wang P, Zhang LM, Xie YZY, et al. Heat waves in China: Definitions, leading patterns, and connections to large-scale atmospheric circulation and SSTs. Adv Sci. 2017;4:10.
8. Stewart IT, Rogers J, Graham A. Water security under severe drought and climate change: Disparate impacts of the recent severe drought on environmental flows and water supplies in Central California. J Hydrol X. 2020;7:100054.
9. Wang F, Wang Z, Yang H, et al. Utilizing GRACE-based groundwater drought index for drought characterization and teleconnection factors analysis in the North China Plain. J Hydrol. 2020;585:124849.
10. Schuldt B, Buras A, Arend M, et al. A first assessment of the impact of the extreme 2018 summer drought on Central European forests. Basic Appl Ecol. 2020;45:86.
11. Steele-Dunne SC, Hahn S, Wagner W, et al. Investigating vegetation water dynamics and drought using Metop ASCAT over the North American Grasslands. Remote Sens Environ. 2019;224:219–235.
12. Qian X, Qiu B, Zhang Y. Widespread decline in vegetation photosynthesis in Southeast Asia due to the prolonged drought during the 2015/2016 El Niño. Remote Sens. 2019;11:910.
13. Zhang Y, Joiner J, Gentine P, et al. Reduced solar-induced chlorophyll fluorescence from GOME-2 during Amazon drought caused by dataset artifacts. Glob Chang Biol. 2018;24):2229–2230.
14. Yuan W, Cai W, Chen Y, et al. Severe summer heatwave and drought strongly reduced carbon uptake in Southern China. Sci Rep. 2016;6: 18813.
15. Yu X, Wang Y, Yu S, et al. Synchronous droughts and floods in the Southern Chinese Loess Plateau since 1646 CE in phase with decadal solar activities. Glob Planet Change. 2019;183:103033.
16. Zhang Q, Yu H, Sun P, et al. Multisource data based agricultural drought monitoring and agricultural loss in China. Glob Planet Change. 2019; 172:298–306.
17. Chiogna G, Skrobanek P, Narany TS, et al. Effects of the 2017 drought on isotopic and geochemical gradients in the Adige catchment, Italy. Sci Total Environ. 2018;645:924–936.
18. Yang W, Tan B, Huang D, et al. MODIS leaf area index products: From validation to algorithm improvement. IEEE Trans Geosci Remote Sens. 2006;44:1885–1898.
19. Nanzad L, Zhang J, Tuvdendorj B, et al. NDVI anomaly for drought monitoring and its correlation with climate factors over Mongolia from 2000 to 2016. J Arid Environ. 2019;164:69–77.
20. Sweet SK, Wolfe DW, DeGaetano A, et al. Anatomy of the 2016 drought in the Northeastern United States: Implications for agriculture and water resources in humid climates. Agric For Meteorol. 2017;247:571–581.
21. Anwaar HA, Perveen R, Mansha MZ, et al. Assessment of grain yield indices in response to drought stress in wheat (*Triticum aestivum* L.). Saudi J Biol Sci. 2020;27:1818–1823.
22. Stephenson NL, Das AJ, Ampersee NJ, et al. Patterns and correlates of giant sequoia foliage dieback during California's 2012–2016 hotter drought. For Ecol Manage. 2018;419–420:268–278.
23. Park S, Kang D, Yoo C, et al. Recent ENSO influence on East African drought during rainy seasons through the synergistic use of satellite and reanalysis data. ISPRS J Photogramm Remote Sens. 2020;162: 17–26.
24. Yoshida Y, Joiner J, Tucker C, et al. The 2010 Russian drought impact on satellite measurements of solar-induced chlorophyll fluorescence: Insights from modeling and comparisons with parameters derived from satellite reflectances. Remote Sens Environ. 2015;166:163–177.
25. Gonçalves NB, Lopes AP, Dalagnol R, et al. Both near-surface and satellite remote sensing confirm drought legacy effect on tropical forest leaf phenology after 2015/2016 ENSO drought. Remote Sens Environ. 2020; 237:111489.
26. West H, Quinn N, Horswell M. Remote sensing for drought monitoring & impact assessment: Progress, past challenges and future opportunities. Remote Sens Environ. 2019;232:111291.
27. Mohammed GH, Colombo R, Middleton EM, et al. Remote sensing of solar-induced chlorophyll fluorescence (SIF) in vegetation: 50 years of progress. Remote Sens Environ. 2019;231:111177.
28. Li Z, Zhang Q, Li J, et al. Solar-induced chlorophyll fluorescence and its link to canopy photosynthesis in maize from continuous ground measurements. Remote Sens Environ. 2020;236:111420.
29. Liu W, Atherton J, Mõttus M, et al. Simulating solar-induced chlorophyll fluorescence in a boreal forest stand reconstructed from terrestrial laser scanning measurements. Remote Sens Environ. 2019;232:111274.
30. Biriukova K, Celesti M, Evdokimov A, et al. Effects of varying solar-view geometry and canopy structure on solar-induced chlorophyll fluorescence and PRI. Int J Appl Earth Obs Geoinf. 2020;89:102069.
31. Peng B, Guan K, Zhou W, et al. Assessing the benefit of satellite-based Solar-Induced Chlorophyll Fluorescence in crop yield prediction. Int J Appl Earth Obs Geoinf. 2020;90:102126.
32. Fu P, Meacham-Hensold K, Siebers MH, et al. The inverse relationship between solar-induced fluorescence yield and photosynthetic capacity: Benefits for field phenotyping. J Exp Bot. 2021;72:1295–1306.
33. Joiner J, Guanter L, Lindstrot R, et al. Global monitoring of terrestrial chlorophyll fluorescence from moderate-spectral-resolution near-

infrared satellite measurements: Methodology, simulations, and application to GOME-2. Atmos Meas Tech. 2013;6:2803–2823.
34. Somkuti P, Bösch H, Feng L, et al. A new space-borne perspective of crop productivity variations over the US Corn Belt. Agric For Meteorol. 2020; 281:107826.
35. Frankenberg C, Fisher JB, Worden J, et al. New global observations of the terrestrial carbon cycle from GOSAT: Patterns of plant fluorescence with gross primary productivity. Geophys Res Lett. 2011;38: L17706.
36. Sun Y, Frankenberg C, Jung M, et al. Overview of solar-induced chlorophyll fluorescence (SIF) from the orbiting carbon observatory-2: Retrieval, cross-mission comparison, and global monitoring for GPP. Remote Sens Environ. 2018;209:808–823.
37. Meroni M, Atzberger C, Vancutsem C, et al. Evaluation of agreement between space remote sensing SPOT-VEGETATION fAPAR time series. IEEE Trans Geosci Remote Sens. 2013;51:1951–1962.
38. Amoros-Lopez J, Gomez-Chova L, Vila-Frances J, et al. Evaluation of remote sensing of vegetation fluorescence by the analysis of diurnal cycles. Int J Remote Sens. 2008;29:5423–5436.
39. Papageorgiou GC, Govindjee G. Chlorophyll a fluorescence: A signature of photosynthesis. Dordrecht: Kluwer (now Springer), 2004.
40. Govindjee G, Amesz J, Fork DC. Light emission by plants and bacteria. Orlando: Academic Press, 1986.
41. Wang S, Zhang Y, Ju W, et al. Warmer spring alleviated the impacts of 2018 European summer heatwave and drought on vegetation photosynthesis. Agric For Meteorol. 2020;295:108195.
42. Chen S, Huang Y, Wang G. Detecting drought-induced GPP spatiotemporal variabilities with sun-induced chlorophyll fluorescence during the 2009/2010 droughts in China. Ecol Indic. 2021;121:107092.
43. Wen J, Köhler P, Duveiller G, et al. A framework for harmonizing multiple satellite instruments to generate a long-term global high spatial-resolution solar-induced chlorophyll fluorescence (SIF). Remote Sens Environ. 2020;239:111644.
44. Wang N, Suomalainen J, Bartholomeus H, et al. Diurnal variation of sun-induced chlorophyll fluorescence of agricultural crops observed from a point-based spectrometer on a UAV. Int J Appl Earth Obs Geoinf. 2021; 96:102276.
45. Wang J, Wu C, Zhang C, et al. Improved modeling of gross primary productivity (GPP) by better representation of plant phenological indicators from remote sensing using a process model. Ecol Indic. 2018;88: 332–340.
46. Fu X, Tang C, Zhang X, et al. An improved indicator of simulated grassland production based on MODIS NDVI and GPP data: A case study in the Sichuan province, China. Ecol Indic. 2014;40:102–108.
47. Gonsamo A, Chen JM, Price DT, et al. Land surface phenology from optical satellite measurement and CO2 eddy covariance technique. J Geophys Res Biogeosciences. 2012;117, DOI: 10.1029/2012JG002070.
48. Jeong S-J, Schimel D, Frankenberg C, et al. Application of satellite solar-induced chlorophyll fluorescence to understanding large-scale variations in vegetation phenology and function over northern high latitude forests. Remote Sens Environ. 2017;190:178–187.
49. Cescatti A, Marcolla B, Vannan SKS, et al. Intercomparison of MODIS albedo retrievals and *in situ* measurements across the global FLUXNET network. Remote Sens Environ. 2012;121:323–334.
50. Damm A, Guanter L, Verhoef W, et al. Impact of varying irradiance on vegetation indices and chlorophyll fluorescence derived from spectroscopy data. Remote Sens Environ. 2015;156:202–215.
51. Guanter L, Aben I, Tol P, et al. Potential of the TROPOspheric Monitoring Instrument (TROPOMI) onboard the Sentinel-5 Precursor for the monitoring of terrestrial chlorophyll fluorescence. Atmos Meas Tech. 2015;8: 1337–1352.
52. Wagle P, Xiao X, Suyker AE. Estimation and analysis of gross primary production of soybean under various management practices and drought conditions. ISPRS J Photogramm Remote Sens. 2015;99: 70–83.
53. Pei W, Fu Q, Liu D, et al. Spatiotemporal analysis of the agricultural drought risk in Heilongjiang Province, China. Theor Appl Climatol. 2018; 133:151–164.
54. Wang J, Huang X, Zhong T, et al. Climate change impacts and adaptation for saline agriculture in north Jiangsu Province, China. Environ Sci Policy. 2013;25:83–93.
55. Lu E, Liu S, Luo Y, et al. The atmospheric anomalies associated with the drought over the Yangtze River basin during spring 2011. J Geophys Res Atmos. 2014;119:5881–5894.
56. Vicente-Serrano SM, Beguería S, López-Moreno JI. A multiscalar drought index sensitive to global warming: The standardized precipitation evapotranspiration index. J Clim. 2010;23:1696–1718.
57. Joiner J, Yoshida Y, Guanter L, et al. New methods for the retrieval of chlorophyll red fluorescence from hyperspectral satellite instruments: Simulations and application to GOME-2 and SCIAMACHY. Atmos Meas Tech. 2016;9:3939–3967.
58. Frankenberg C, Berry J. Solar induced chlorophyll fluorescence: Origins, relation to photosynthesis and retrieval. Compr Remote Sens. 2018;3: 143–162.
59. Köhler P, Guanter L, Joiner J. A linear method for the retrieval of sun-induced chlorophyll fluorescence from GOME-2 and SCIAMACHY data. Atmos Meas Tech. 2015;8:2589–2608.
60. Guanter L, Zhang Y, Jung M, et al. Global and time-resolved monitoring of crop photosynthesis with chlorophyll fluorescence. Proc Natl Acad Sci. 2014;111:E1327—E1333.
61. Li X, Xiao J, He B, et al. Solar-induced chlorophyll fluorescence is strongly correlated with terrestrial photosynthesis for a wide variety of biomes: First global analysis based on OCO-2 and flux tower observations. Glob Chang Biol. 2018;24:3990–4008.
62. Zhang Y, Xiao X, Jin C, et al. Consistency between sun-induced chlorophyll fluorescence and gross primary production of vegetation in North America. Remote Sens Environ. 2016;183:154–169.

**Cite this article as:** Pandiyan S, Govindjee G, Meenatchi S, Prasanna S, Gunasekaran G, Guo Y (2021) Evaluating the impact of summer drought on vegetation growth using space-based solar-induced chlorophyll fluorescence across extensive spatial measures. *Big Data* X:X, 1–16, DOI: 10.1089/big.2020.0350.

## Abbreviations Used

$\Phi_F$ = SIF normalized by APAR
$\Omega_C$ = escape eventuality binding the discharge of fluorescence from the top of the canopy to the emission of fluorescence
APAR = absorbed photosynthetically active radiation
EVI = enhanced vegetation index
fPAR = fraction of APAR
GOME-2 = Global Ozone Monitoring Instrument-2
GPP = gross primary productivity
LAI = leaf area index
MODIS = Moderate Resolution Imaging Spectroradiometer
NDVI = normalized difference vegetation index
OCO-2 = Orbiting Carbon Observatory-2
PAR = photosynthetically active radiation
SIF = solar-induced chlorophyll fluorescence
$SIF_{PAR}$ = SIF normalized by PAR
SM = soil moisture
SPEI = standardized precipitation evapotranspiration index
VIs = vegetation indices